Unexpected Resistance of Polyelectrolyte Brushes Formed via Surface-Initiated Polymerization on Glass and Sitall

O. Izhyk[a,*], O. Balaban[a], N. Mitina[b],
K. Volianiuk[b], Kh. Harhay[b],
I. Grygorchak[a] and A. Zaichenko[a,b]

[a]*Department of Applied Physics and Nanomaterials Science,
Lviv Polytechnic National University, Ustyianovycha 5, 79013 Lviv, Ukraine*
[b]*Department of Organic Chemistry, Lviv Polytechnic National University,
Svyatyi Yuriy sq. 2, 79013 Lviv, Ukraine*

Poly(dimethylaminoethyl methacrylate) and poly(2-carboxyethyl acrylate) brushes, including enriched with Li^+ cations, were grafted to the glass and glass-ceramic via radical polymerization initiated by immobilized low molecular weight 4,4'-azobis (4-cyanopentanoic acid) and multi-site oligoperoxide metal complex initiators. The atomic force microscopy method was used to characterize and determine the thickness of polymer layers. Surface tension and contact angle of modified substrates were studied using contact angle measurements. It was revealed that resistance properties of grafted brushes studied in the frequency range 10^{-3}–10^6 Hz by impedance spectroscopy depend on the initiator, substrate, and polymer natures and can be explained by the formation of polymer brushes of different packing densities on the substrates. It was assumed that 4–6 orders falling values of resistance observed for "grafting from" polyelectrolyte brushes initiated by 4,4'-azobis (4-cyanopentanoic acid) on glass substrate was caused by proton conductivity.

topics: polyelectrolyte brush, proton conductivity, impedance, atomic force microscopy (AFM)

1. Introduction

The development of a tunable method for preparing power sources and energy storage is a perspective way to provide the maximum energy density, high efficiency, eco-friendliness and other necessary properties for such devices. Optimization of the batteries with high capacity obviously should be done on the molecular level. Using for this aim polymer brushes, possessing unique properties and broad applications such as nanoparticle stabilization, stimuli-responsive surfaces, polymer ionic liquids and organic solar cells, seems to be a reasonable choice [1]. Polymer brushes are used in organic batteries, for thin-film cathodes, for adhesion and capacitance improvement in silicon, carbon-based electrodes, and MoS_2 nanocomposites [2]. Moreover, polymer brushes provide surface conductivity in a dry state, which is promising for the development of solid-state batteries, batteries-on-chip technologies, and stretchable supercapacitors [3, 4]. A low energy density, self-discharge, low ion diffusion, changing the porosity,

blocking ion penetration, and dissolution of the polymer in the electrolyte are disadvantages of their applications [5, 6]. It caused the necessity to synthesize polymer brushes possessing controlled electrophysical properties. Surface initiated graft-polymerization is one of the most perspective ways for the construction of functional polymer brushes. The nature of immobilized initiators and monomers, as well as polymerization techniques, define the length, packing density, surface morphology and surface energy of grafted polyelectrolyte brushes and as a result, control ion pathways and surface conductivity. Such an approach provides surface immobilization of polymer layer in porous media that increase the specific capacitance of the cathodes materials [7, 8].

The aim of the work is to construct the polyelectrolyte brushes of cationic and anionic type via the "grafting from" method and to study the modified surface properties. The formation of a homogeneous layer of polyelectrolyte brushes with controlled packing density, thickness and ions diffusion paths is considered in this work.

2. Experimental

2.1. Materials

The glass slides (size 25×75 mm^2) purchased from Skloprylad (Kharkiv, Ukraine) and aluminum oxide (sitall) polished slides (size 15×35 mm^2) obtained from Zakhidprylad (Lviv, Ukraine) were used in this work. The initiators of radical polymerization were: oligoperoxide metal complex (OMC) synthesized via polymerization of vinyl acetate (VA), 5-tertbutylperoxy-5-methyl-1-hexen-3-yne (VEP) maleic acid (MA) and further coordination with Cu^{2+} cations as described [9], and 4,4'-azobis (4-cyanopentanoic acid) (ACPA) purchased from Sigma-Aldrich. Monomers, 2-(dimethylamino)ethyl methacrylate (DMAEMA) and 2-carboxyethyl acrylate (CEA), were purchased from Sigma-Aldrich. Lithium chloride (LiCl·H$_2$O), γ-aminopropyl triethoxysilane (APTES) and all organic solvents (acetone, isopropanol, methanol) were obtained from Sigma-Aldrich and used without purification.

2.2. Methods

First, the glass and sitall slides were carefully cleaned with acetone and isopropanol. Then amino-modified substrates were obtained by immersion in APTES solution (1% in methanol) at 20°C for 2 h. Afterward, the aminosilanized slides were placed in a 1% acetone solution of OMC or ACPA initiators for 2 h at 20°C. The surface-initiated radical polymerization of DMAEMA and CEA (0.5 M solution in isopropanol) was carried out for 8 h at 40°C for OMC and 60°C for ACPA. Finally, the plates with poly(DMAEMA) and poly(CEA) polymer brushes were salted with LiCl (0.5% in ethanol) for 2 h at 20°C to incorporate Li$^+$ ions. On each step, samples were washed with isopropanol and acetone to eliminate residual reagents. The substrates dried under the ambient conditions at room temperature till constant weight.

2.3. Characterization of materials

The topology and thickness of immobilized polymer brushes were determined using the atomic force microscopy (AFM) technique (Solver P47-PRO, NT MTD Spectrum Instruments). Impedance spectroscopy was made using measuring complex Autolab (MetrohmAutolab B.V., The Netherlands). Measurements of the surface resistance were made in the frequency range of 10^{-2}–10^5 Hz at 20°C in air by using silver contacts placed 1 cm from each other on the front side of the sample surface. The amplitude of the measuring signal was 5×10^{-3} V. The Dirichlet filter was used for the removal of doubtful points. Errors of approximation did not exceed 4%. Wetting properties of the surfaces were estimated using water and diiodomethane for contact angle measurements. The measurements were carried out under ambient conditions at 20°C and 42% relative humidity. Photos of the simple static drop were recorded by USB microscope Ootdty DM-1600 and processed by the ImageJ plugin. An averaged contact angle was calculated by root mean square of 8–10 measurements.

3. Results and discussion

3.1. Study of polyelectrolyte modified ceramic surfaces

In Fig. 1, one can see that as a result of radical graft-polymerization of DMAEMA and CEA initiated by ACPA or multi-site oligoperoxide OMC immobilized on slide surface, nanolayers of grafted polyelectrolyte brushes are formed. AFM images demonstrate thin and relatively smooth brushes of poly(DMAEMA) and poly(CEA) covalently attached to the surface. The thickness of both polyelectrolyte brushes depends on substrate nature and reaches 15–30 nm for sitall and much more, i.e., up to 500 nm, for glass.

Moreover, one can see different surface packing densities of the brushes depending on substrate type. The results of the water contact angle (WCA) study of the modified glass substrate and surface tension (γ) calculated by the Owens-Wendt approach demonstrate a higher value of WCA (76°) on glass with APTES as a precursor in comparison with clean glass (22°) and the surface tension γ of 41 mN/m.

A small deviation from the average WCA declares the formation of a smooth and homogeneous layer with strong covalent –Si–O–Si–O– hydrophobic bonding. WCA for plates modified with multi-site and more hydrophobic initiator OMC increases at 6°, while for ACPA, it decreases at 6°. "Grafting from" poly(DMAEMA) and poly(CEA) brushes reduces water contact angle even more.
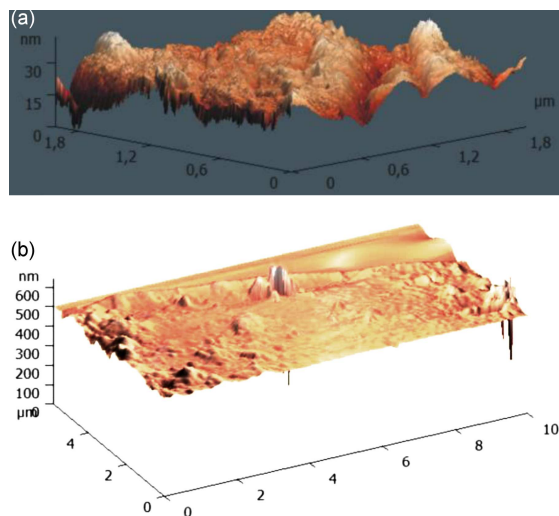

Fig. 1.   AFM images of (a) poly(DMAEMA), and (b) poly(CEA) brushes on sitall and glass.

Wetting properties. Here, γ_d denotes dispersive forces, γ_n — non-dispersive forces, and γ — total surface tension.

#	Polymer	Water contact angle (WCA) [°]	Surface tension [mN/m]		
			γ_d	γ_n	γ
APTES		76.2 ± 1.5	34.6 ± 1	6.1 ± 0.7	40.7 ± 1.6
OMC		82.3 ± 1.0	31.8 ± 1.4	4.4 ± 0.7	36.2 ± 2.2
	poly(DMAEMA)	71.5 ± 4.3	33.5 ± 1.8	8.6 ± 2.7	42.1 ± 4.5
	poly(CEA)	69.9 ± 1.4	33.1 ± 1	9.5 ± 1.1	42.6 ± 2.1
ACPA		70.3 ± 1.5	32.0 ± 2.1	9.7 ± 1.5	41.8 ± 3.6
	poly(DMAEMA)	67.9 ± 2.2	37.0 ± 1	9.2 ± 1.4	46.2 ± 2.4
	poly(CEA)	68.1 ± 3.5	34.5 ± 1.1	10.0 ± 2.2	44.5 ± 3.3

In general, this is observed for both immobilized initiators, however, the WCA value for OMC (11°) due to its multi-site and, possibly, more hydrophobic nature is more convincing than for ACPA (2°). Compared to the initial APTES layer, polymer brushes are characterized by insignificantly higher surface tension. Most likely, attached polymer chains form mushroom-like coverings on the surface. That, evidently, causes a high enough influence of previous precursor layers on wetting properties.

3.2. Study of resistance of polyelectrolyte coated substrates

The results of the AFM and contact angle study show that the formation of bilayer structures APTES/polyelectrolyte is irreversibly attached to the glass or sitall planar surface (Table I, Fig. 1). The results of surface resistance measurements presented as dependences of the real part of the complex impedance on the frequency $\mathrm{Re}(Z(f))$ (Figs. 2 and 3) demonstrate that (i) as expected, the value of $\mathrm{Re}((Z(f))$ depends on the substrate type (Fig. 2), and is higher for glass than for sitall slides covered by APTES (this clearly relates to the initial slide surface relief that influences the polymer layer growth and topology); (ii) a surface modified with APTES is dielectric with an insignificant contribution of the localized carriers to the passage of currents [10] (quasi-horizontal region of $\mathrm{Re}(Z(f))$ dependence in the lowest frequency region) (Fig. 2, curves 1, 8). With increasing frequency, the value of $\mathrm{Re}(Z(f))$ decreases due to the contribution of the delocalized carriers from the trap centers near the Fermi level and as a result of the displacement currents [11].

The impact of the substrate on the current passage is observed clearly after the poly(CEA) grafting via radical polymerization (Fig. 2, curves 2, 9) initiated by ACPA. However, the resistance (curve 9) of the poly(CEA) brushes grafted to the sitall slide remains almost the same as for the initial APTES layer on sitall (Fig. 2, curve 8), while it decreases up to 6 orders of magnitude on the glass slide (Fig. 2, curve 2). Moreover, its frequency dependence indicates the ion conduction mechanism
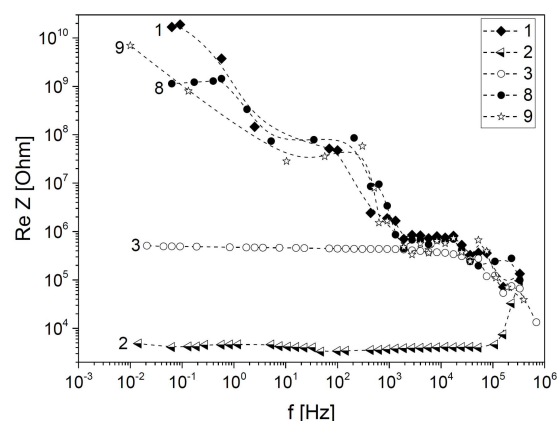

Fig. 2. Impedance real part $\mathrm{Re}(Z(f))$. Samples on glass substrate: 1 — APTES; 2 — CEA initiated by ACPA (ACPA–CEA); 3 — ACPA–DMAEMA. Samples on sitall substrate: 8 — APTES; 9 — ACPA–CEA.

(carriers are delocalized released ions) (Fig. 2, curve 2). In our opinion, the increase of $\mathrm{Re}(Z(f))$ at frequencies above 10^5 Hz is the evidence of the devastation of trap centers near the Fermi level.

A similar dependence of $\mathrm{Re}(Z(f))$ was revealed after the "grafting from" poly(DMAEMA) brushes initiated by ACPA (Fig. 2, curve 3). The resistance of the latter was 4 orders lower in comparison with the resistance value of APTES only coated slide (Fig. 2, curve 1) but 2 orders higher than the resistance of poly(CEA) brushes (Fig. 2, curve 2). Such a phenomenon is caused, in our opinion, by proton carriers trapped between brushes. We assume that, due to the hydrogen bond formation, poly(CEA) and poly(DMAEMA) brushes produce an efficient source of H^+ cations localized around carboxyl group or nitrogen atom and, as a result, increase the surface conductivity. Moreover, both poly(DMAEMA) and poly(CEA) brushes can contain some amount of water molecules bound through the formation of hydrogen bonds with polyelectrolyte polar groups. And it probably also contributes to the appearance of conductivity of the materials (Fig. 2, curves 2, 3).
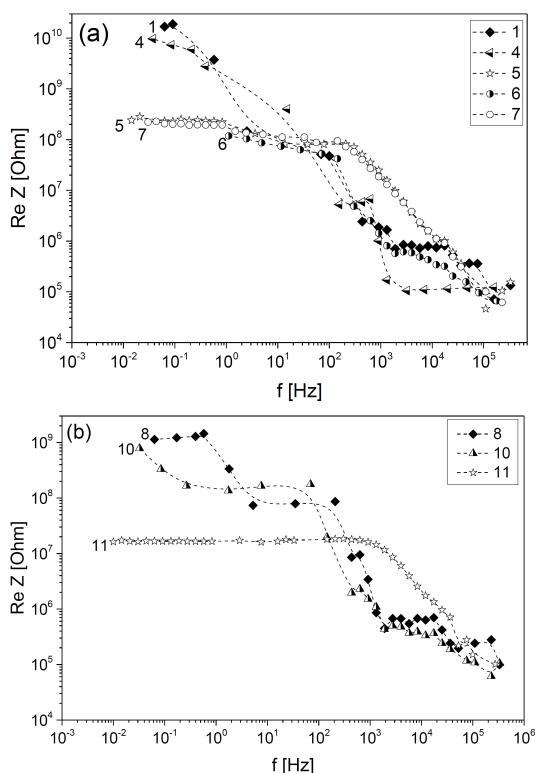
Fig. 3. Impedance real part $\text{Re}((Z(f))$. (a) Samples on glass substrate: 1 — APTES; 4 — CEA initiated by OMC (OMC–CEA); 5 — OMC–CEA after treatment with LiCl (OMC–CEA–LiCl); 6 — OMC–DMAEMA; 7 — OMC–DMAEMA–LiCl. (b) Samples on sitall substrate: 8 — APTES; 10 — OMC–CEA; 11 — OMC–CEA–LiCl.

The inclusion of Li$^+$ cations via processing the grafted polyelectrolyte brushes with LiCl does provide 2 orders of magnitude reduction of resistance in poly(CEA) or poly(DMAEMA) on both glass and sitall substrates (Fig. 3, curves 5, 7, 11). However, the effect of obtaining the resistance in the frequency range 10^2–10^5 Hz was unexpected. It can be assumed that the treatment of the OMC–poly(CEA) and OMC–poly(DMAEMA) brushes (Fig. 3, curves 5, 7, 11) with LiCl solution impedes the proton conductivity caused by the vacancy jumping due to binding Cl$^-$ anions to H$^+$–Cl$^-$ proton–anion pairs.

The resistance of grafted brushes on sitall substrate (Fig. 2, curve 9) differs slightly from that of the pre-modified substrates with APTES only (Fig. 2, curves 1, 8), as was mentioned before. This, evidently, is explained by the peculiarities of the formation of polymer brushes on the sitall substrate. Low molecular weight ACPA molecules cannot provide grafting polymer brushes with the packing density on sitall substrate sufficient for the shortest ion pathways. The formation of the ACPA–poly(CEA) brushes of higher packing density on glass (curve 2), on the contrary, contributes to conductivity.

Larger molecules of oligoperoxide OMC initiator are not strictly dependent on the substrate type (Fig. 3, curves 4, 6, 10) because the packing density of the grafted polyelectrolyte molecules is defined predominantly by the amount and localization of OMC radical forming sites of initiated radical polymerization. That explains the conformity of the shapes of the $\text{Re}((Z(f))$ curves for OMC–poly(CEA) on the glass or sitall (curves 4, 10). One can also see (curve 10) that one order increase in conductivity appears for OMC–CEA on the glass substrate in 10^3–10^5 Hz, while for an OMC–CEA sitall substrate, it appears at infralow frequencies.

4. Conclusions

"Grafting from" polyelectrolyte poly(DMAEMA) and poly(CEA) brushes to sitall and glass substrates via surface-initiated polymerization provides visible change of the surface relief, wetting and resistance characteristics. Their thickness on glass was above 16 times (500 nm) higher than (15–30 nm) on sitall. An unexpected conductivity in a dry state of poly(DMAEMA) and poly(CEA) brushes grafted to sitall and glass substrates was revealed. It is assumed that this phenomenon is caused mainly by proton carriers trapped between brushes. The increase in resistance of poly(CEA) brushes grafted to glass modified by OMC is observed in the frequency range 10^2–10^4 Hz, after treating the brushes with LiCl solution, due to binding Cl$^-$ anions into H$^+$–Cl$^-$ proton–anion pairs. The values of resistance of the brushes depend on the used initiator, the substrate, as well as the polyelectrolyte nature, which define the density of the polymer brush packing and interaction between chains on the surfaces. For the ACPA initiator, the highest packing density, which contributes to conductivity, is obtained on glass. This dependence is not so significant for the OMC initiator, since the packing density of grafted molecules is defined predominantly by the amount of oligoperoxide initiating centers of radical polymerization compared to the impact of the substrate.

References

[1] D. Mecerreyes, *Prog. Polym. Sci.* **36**, 1629 (2011).

[2] O. Balaban, N. Mitina, A. Zaichenko, O. Paiuk, Y. Shermolovich, in: *2020 IEEE 10th Int. Conf. Nanomaterials: Applications & Properties (NAP)*, 2020, p. 02NEE14.

[3] Q. Zhao, S. Stalin, C.-Z. Zhao, L.A. Archer, *Nat. Rev. Mater.* **53**, 229 (2020).

[4] W. Wu, *Sci. Technol. Adv. Mater.* **20**, 187 (2019).

[5] Y.H. Wang, M.K. Hung, C.H. Lin, H.C. Lin, J.T. Lee, *Chem. Commun.* **47**, 1249 (2011).

[6] M.D. Hager, B. Esser, X. Feng, W. Schuhmann, P. Theato, U.S. Schubert, *Adv. Mater.* **32**, 1 (2020).

[7] B.H. Shen, G.M. Veith, W.E. Tenhaeff, *Sci. Rep.* **8**, 1 (2018).

[8] C. Li, S. Liu, C. Shi, G. Liang, Z. Lu, R. Fu, D. Wu, *Nat. Commun.* **101**, 1 (2019).

[9] A. Kostruba, A. Zaichenko, N. Mitina, K. Rayevska, K. Hertsyk, *Cent. Eur. J. Phys.* **6**, 454 (2008).

[10] M. Pollak, T.H. Geballe, *Phys. Rev.* **122**, 1742 (1961).

[11] O.V. Balaban, I.I. Grygorchak, A.I. Kondyr, O.S. Zaichenko, N.E. Mitina, V.V. Datsyuk, S.E. Trotsenko, O.S. M'yahkota, *Mater. Sci.* **53**, 179 (2017).